2024 IEEE/RSJ International Conference on Intelligent Robots and Systems (IROS)
October 14-18, 2024. Abu Dhabi, UAE

Non-Repetitive: A Promising LiDAR Scanning Pattern

Angchen Xie Yeqiang Qian* Weihao Yan Chunxiang Wang Ming Yang

***Abstract*— LiDAR is an essential sensor for intelligent vehicles. Recently, LiDARs used in vehicles produced by different companies have significant differences in their scanning patterns. Some vehicles use mechanical and solid-state (repetitive) LiDARs, while others use prism-based (non-repetitive) LiDARs. The scanning pattern of a LiDAR has a profound impact on its scanning performance. To investigate the influence of LiDAR scanning patterns, we created the "Repetitive-or-not" dataset, which is collected simultaneously by LiDARs with both repetitive and non-repetitive scanning patterns in the CARLA simulation environment. Using this dataset, we conducted a comprehensive statistical analysis of the scanning ability of repetitive and non-repetitive LiDARs. Furthermore, we looked into the effects of these two LiDAR scanning patterns on the performance of various 3D object detection algorithms. Finally, we explored the domain gap in the point cloud data produced by repetitive and non-repetitive LiDARs. Through an in-depth investigation of the "Repetitive-or-not" dataset, we have discovered that non-repetitive LiDAR shows great promise. This conclusion is primarily supported by its superior object scanning capabilities.**

I. Introduction

LiDAR is one of the most popular sensors in autonomous vehicles, providing real-time data about the surrounding environment. Its adoption has rapidly accelerated the development of self-driving technology [1], and now automotive companies are embracing industrial-grade LiDAR systems.

In the surge of developments in the autonomous driving industry over the past decade, the widely accepted form of LiDARs has long been the mechanical and solid-state (repetitive) LiDAR [2]–[4]. However, during the CES exhibition in 2020, Livox introduced the Horizon, bringing a new paradigm to the field of autonomous driving perception: non-repetitive scanning, which is based on a rotating prism. Figure 1 shows the differences between these two scanning patterns and point cloud they produced. Repetitive scanning leads to a high duplication of point clouds in neighboring frames, while non-repetitive scanning produces point clouds with varying shapes from frame to frame. As shown in Table I, both repetitive and non-repetitive LiDARs are prevalent in commercially available vehicle models.

To investigate the impact of different LiDAR scanning patterns on the perception module of autonomous driving, we collected a dataset called "Repetitive-or-not" using both repetitive and non-repetitive LiDAR simultaneously in the CARLA [5] simulation environment. This dataset features a variety of typical highway and urban scenarios. To facilitate academic research, we have open-sourced this dataset for interested researchers to use. The dataset is available on *https://www.kaggle.com/datasets/angchenxie/repetitive-or-not*

Based on the "Repetitive-or-not dataset", we conducted a study on the scanning abilities of LiDARs from two perspectives. Firstly, we analyzed LiDAR's overall ability to capture environmental objects, specifically the quality of environmental objects that LiDARs can detect. In the second phase, we examined the performance of perception tasks on objects captured by LiDARs and measured the differences caused by different scanning patterns. Our experiment focused on the classic 3D object detection task across all perception tasks. To get more comprehensive results, we have meticulously selected diverse 3D object detection algorithms, which are based on multiple feature extraction methods,

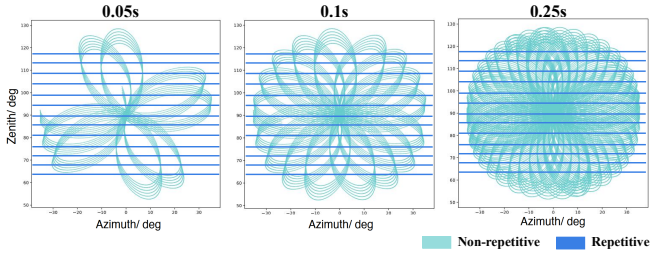

(a) Laser beam distribution

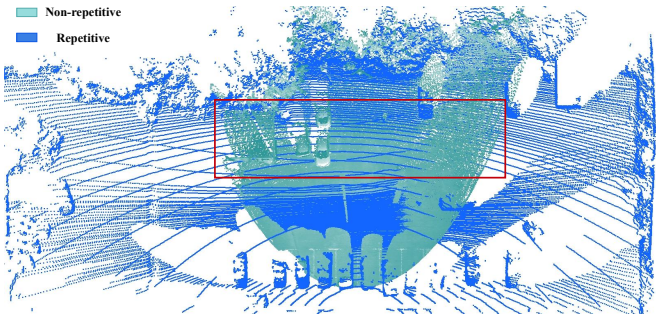

(b) Visualization of point clouds

Fig. 1: (a) illustrates the distribution of laser beams emitted by LiDARs with different scanning patterns over time. As time increases, the coverage of the laser beams emitted by the non-repetitive LiDAR becomes denser, whereas that of repetitive LiDAR remains constant. (b) illustrates point clouds collected by different LiDARs in the same scene, with the red box representing overlaps.

This work was supported by the National Natural Science Foundation of China (62103261/62173228/U22A20100/62373250).

All the authors are with the Department of Automation, Shanghai Jiao Tong University, Shanghai, 200240, China; also with Key Laboratory of System Control and Information Processing, Ministry of Education of China, Shanghai, 200240, China.

*Corresponding author: Yeqiang Qian (e-mail: qianyeqiang@sjtu.edu.cn).

TABLE I: LiDAR types and parameter configurations for different brands of vehicle models.

Type	Company	Model	Distance	Resolution	Points/s
Repetitive	Hesai	Ideal MEGA	200m	$0.1^\circ \times 0.2^\circ$	1,536,000
	Robosence	AION LX Plus	200m	$0.2^\circ \times 0.2^\circ$	787,500
	Huawei	Luxeed S7	250m	$0.1^\circ \times 0.1^\circ$	1,840,000
Non-repetitive	Livox	Xpeng P5	150m	$0.18^\circ \times 0.23^\circ$	452,000

for performance evaluation on our dataset. This allowed us to assess the impact of different scanning patterns on the performance of 3D object detection algorithms.

The contributions of this study can be summarized as follows:

- We curated the "Repetitive-or-not" dataset, which considers LiDAR scanning patterns as the only variable. The dataset includes urban and highway scenarios and has three categories: vehicles, cyclists, and pedestrians. This dataset serves as a valuable resource for future research on LiDAR scanning patterns.
- We conducted a comprehensive investigation into the scanning capabilities of LiDARs with repetitive and non-repetitive scanning patterns in both urban and highway scenarios. Based on our extensive experiments, we have concluded that non-repetitive LiDAR exhibits greater promise due to its superior scanning abilities.
- We analyzed the performance of various 3D object detection algorithms between repetitive and non-repetitive data, as well as the domain gap resulting from these two LiDAR scanning patterns. Our findings demonstrate that the transformer-based model not only achieves superior performance but also exhibits exceptional migration capability between different LiDAR scanning patterns.

II. Related Works

A. 3D Object Detection

Advancements in deep neural networks have greatly improved tasks related to 3D point clouds, including object detection and semantic segmentation [6]–[21]. This paper investigates the impact of repetitive and non-repetitive LiDAR scanning patterns on the detection of 3D objects in outdoor traffic scenarios for autonomous driving.

Inspired by successful indoor methodologies such as [13]–[16], outdoor object detection primarily focuses on identifying vehicles, cyclists, and pedestrians [22]. Various approaches utilizing different data representation paradigms, such as pillar-based [8, 9] and voxel-based [6, 7, 17, 18], transform point clouds into 2D planes or pseudo-3D images. To prevent information loss, PointNet [23] is utilized to directly extract features from points, influencing end-to-end architectures [10, 11] and mixed-data algorithms [19, 20].

The transformer model, which is widely used in natural language processing, has also proven to be effective in computer vision [24]. Among the various transformer-based 3D object detection frameworks for outdoor scenarios, CT3D [12] is particularly noteworthy. It adopts a two-stage approach, using a region proposal network [7] to generate initial boxes, and then incorporating transformers to improve contextual interactions and aggregate features, resulting in highly accurate predictions.

B. Outdoor 3D Point Cloud Dataset

The majority of modern end-to-end 3D object detection algorithms that are focused on outdoor environments rely heavily on authentic outdoor datasets for both training and assessment [3, 4, 25]–[28]. These datasets provide a comprehensive array of data capturing varied real-world scenarios, encompassing diverse road and weather conditions, object classes, and a multitude of detected objects.

However, a notable limitation of these datasets is that LiDARs collected them with the same scanning patterns. In KITTI [25], NuScenes [3], and Waymo [4], point cloud data was only collected by repetitive LiDARs. Additionally, there is a lack of outdoor datasets collected by non-repetitive LiDAR. This poses a challenge in assessing the scanning abilities of LiDARs with different scanning patterns and analyzing the impact of such patterns on 3D object detection.

In our research, we need to use the data with the LIDAR scanning pattern as the only variable to conduct experiments. As outdoor scenarios have varying collection environments, it is not feasible to ensure the production of point cloud data scanned by different LIDARs simultaneously. Therefore, we have opted to collect data using the CARLA simulator and offered researchers the "Repetitive-or-Not" simulation dataset, which compensates for the shortcomings of the current mainstream datasets.

C. Researches on LiDAR Scanning Patterns

Most previous research has categorized LiDAR into three main categories: mechanical, solid-state, and hybrid solid-state [29]. The solid-state category consists mainly of flash-based LiDAR [30] and optical phased array (OPA)-based LiDAR [31], while the hybrid solid-state category includes microelectromechanical system (MEMS)-based LiDAR [32]. Mechanical LiDARs have a physically rotating emission and reception system, which transforms laser points into lines, and multiple laser emitters are arranged vertically to form a plane for 3D scanning. However, these systems have complex internal structures, and are difficult to maintain stable operation for long periods [33]. Flash-based LiDAR captures the entire target scene within a single shot using a photodetector (PD) array. However, the resolution is limited by the physical size of the PD arrays. MEMS mirrors can reduce the size of LiDAR systems and enable solid-state LiDAR scanning, which is compact and lightweight. OPA-based LiDAR uses integrated photonics technology and provides a compact platform. The fabrication of OPA is compatible with complementary metal-oxide-semiconductor (CMOS) processes [34], which reduces the manufacturing cost and opens up more possibilities for the future.

Nevertheless, in our research, we have classified LiDARs based on their scanning patterns, which can be repetitive or

(a) Highway scenario (b) Urban scenario

Fig. 2: The visualization of two scenarios in "Repetitive-or-not" dataset.

TABLE II: Setups for LiDARs used for dataset collection.

Type	Distance	VFOV	HFOV	Points/s	Frequency
Non-repetitive	150m	-15°∼10°	120°	452,000	10Hz
Repetitive	150m	-15°∼10°	120°	452,000	10Hz

non-repetitive. This approach differs from the conventional method of classification that is based on principles. We specifically analyze the distinct point cloud formations that result from these patterns, enabling us to evaluate their performance in different downstream tasks and gain valuable insights for future research and production.

III. The Repetitive-or-not Dataset

We used the CARLA simulation environment to create point clouds captured by both repetitive and non-repetitive LiDAR. We opted for the simulation environment due to the difficulties faced in real-world scenarios where it is impractical to collect data simultaneously under identical conditions for various LiDAR scanning patterns. Additionally, the simulation environment allowed us to efficiently obtain rich data from LiDARs employing different scanning patterns within relatively low time and cost constraints. Furthermore, it provided us with information that may not be obtainable from actual scenarios. For example, unlike datasets collected in real-world scenarios that only record real objects detected by LiDAR, the dataset collected in the simulation environment recorded all objects in the environment. This allowed us to analyze the proportion of objects around the host vehicle that LiDAR can detect. It is important to note that we use the CARLA simulator primarily for its excellent simulation capabilities and support for various scanning patterns of LiDAR. Moreover, it can conveniently generate various traffic participants. Similarly, using simulation environments like Gazebo [35] can also accomplish similar testing and validation.

Specifically, we concurrently collected data frames using both repetitive and non-repetitive LiDAR under identical conditions. To ensure fair data comparisons, we positioned the two LiDARs at the same location and ensured consistency in other parameter configurations, such as field of view, range, acquisition frequency, points collected per second, and so forth. We have outlined the detailed configurations of the two LiDAR setups in Table II. Among them, the non-repetitive LiDAR mainly refers to the parameters of the Livox-HAP LiDAR[1].

As shown in Figure 2, our dataset covers two typical scenarios in autonomous driving: highway and urban environments. The highway section was meticulously collected using the official map "Town04_Opt," which provides a realistic highway setting. We recorded data only relevant to vehicles in the highway section to ensure simplicity in analysis and efficiency. We randomly placed 200 dynamic vehicles on the map, including various types such as cars, trucks, and taxis. The urban section was carefully collected using the official map "Town03_Opt," which offers a comprehensive urban scene. To represent the environment in urban road driving better, we recorded data for three common road participants: vehicles, cyclists, and pedestrians. We randomly placed 120 vehicles, 150 pedestrians, and 60 cyclists on the map. The dataset includes 16,000 frames and is divided into 80 different scenes. Each scene has different environmental settings and includes 200 consecutive data frames.

IV. LiDAR Scanning Ability

In the first stage of our experiments, we aimed to conduct an in-depth comparison of the scanning abilities between repetitive and non-repetitive LiDAR. Our focus was on determining the number of objects (vehicles, cyclists, and pedestrians) that LiDAR could capture in the environment. We defined an object as "hit" if LiDAR captured at least n points from it, and "miss" if not. We varied the value of n to evaluate the quality of the objects captured by LiDAR, using 5, 10, and 15 as the thresholds for low, medium, and high quality, respectively. To avoid counting ground points as object points, we lowered the height of the object's bounding box to 0.05m from the ground. The number and quality of objects detected were then used as the metric to analyze and compare the results in the following experiments.

A. Qualitative Analysis on LiDAR Scanning Ability

In the realm of qualitative analysis, Figure 3 demonstrates the performance of LiDARs in capturing objects under repetitive and non-repetitive scanning patterns. It showcases the bounding boxes of objects that were correctly captured ("hit") and those that were not captured ("missed") when the threshold $n = 5$. The categories of objects represented in the figure are vehicles (in red), cyclists (in blue), and pedestrians (in green). The enclosed regions marked by red circles reveal that non-repetitive LiDARs can detect pedestrians and cyclists that repetitive LiDARs fail to identify. This means that, because of the unique scanning pattern, the non-repetitive LiDAR can cover a more detailed part of the object. So it can capture a more comprehensive point cloud of the same object that is difficult to capture, thus demonstrating the superior scanning abilities of non-repetitive LiDAR.

[1]https://www.livoxtech.com/hap/specs

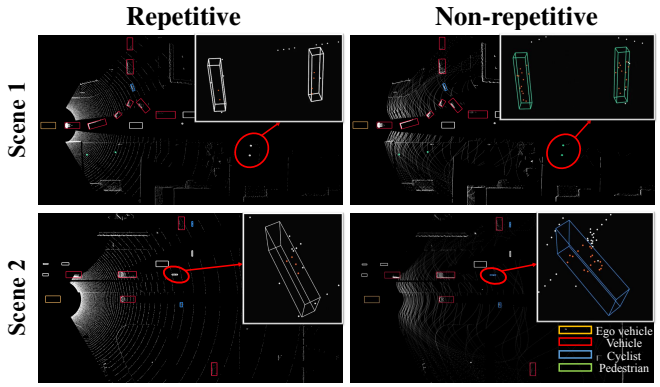

Fig. 3: Visualization of LiDAR point clouds with repetitive and non-repetitive scanning patterns. The arrow indicates an enlarged view of the circled area. In the enlarged view, the orange dots represent the points inside the detection box, while the white dots represent the points outside the detection box.

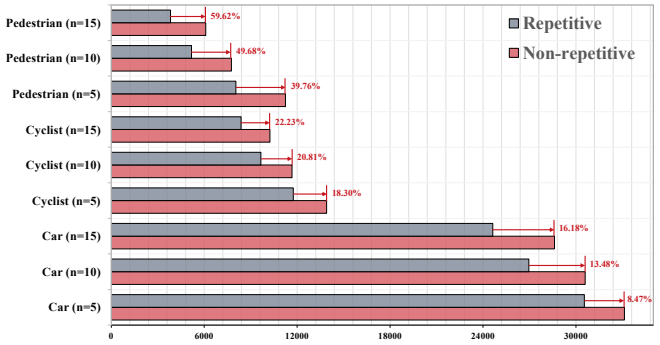

Fig. 4: The number of "hit" vehicles, pedestrians, and cyclists by LiDARs with repetitive and non-repetitive scanning patterns.

B. Quantitative Analysis on LiDAR Scanning Ability

The result of the statistical analysis of the number of environmental objects captured by LiDAR in three quality levels in urban scenes is presented in Figure 4. It is evident that non-repetitive LiDAR can capture more objects than repetitive LiDAR. Additionally, as the object size decreases and the quality levels increase, there is a more significant increase in the number of objects detected by non-repetitive LiDAR. Under the condition of $n = 15$, non-repetitive LiDAR demonstrates a remarkable 59.62% increase in the pedestrian category. Thus, in this section, we can draw the following conclusions:

1) Non-repetitive LiDAR exhibits a superior ability to capture a larger number of objects across all categories in both highway and urban scenarios.
2) Non-repetitive LiDAR demonstrates an even greater capability to capture small objects like pedestrians, offering higher-quality point clouds.

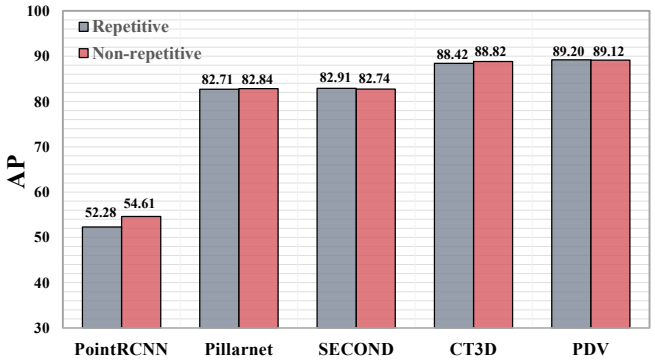

Fig. 5: The performances of different 3D object detection algorithms in the highway scenario under repetitive and non-repetitive LiDAR scanning patterns.

V. Performance of 3D Object Detection Algorithms

In the second stage of our experiments, we utilized objects that were successfully captured by LiDAR as ground truth to train and test multiple 3D object detection algorithms. We aimed to investigate the impact of various point cloud patterns generated from LiDAR with repetitive and non-repetitive scanning patterns on model performance, across different data representation paradigms and backbone architectures. To achieve this goal, we selected specific algorithms for each paradigm: PointRCNN [10] for point-based representation, Pillarnet [9] for pillar-based algorithms, SECOND [7] for voxel-based models, and CT3D [12] and PDV [36] for innovative transformer-based two-stage detectors. Our experiments involved testing the absolute metrics of these algorithms on the "Repetitive-or-not" dataset. Additionally, we explored the potential of model migration from repetitive data to non-repetitive data.

A. Performance of Multiple Algorithms on Repetitive-or-not

1) Highway Scenario: In our experiment on the highway scenario, we focused on inferring and evaluating the category of vehicles. The dataset was divided into 4917 training frames and 2523 testing frames. We excluded 560 frames from the algorithm testing stage because they did not have any vehicles within the specified range. We evaluated the detection results of five 3D object detection models using average precision (AP) as the evaluation metric. It is worth noting that the models were trained and tested on their respective training and testing sets with the same scanning pattern. For instance, we evaluated the results of the "CT3D" model on the "Repetitive" testing frames, having been trained on the "Repetitive" training frames.

We consider the vehicles identified by the algorithm models as true positive (TP) vehicles. In particular, we have defined predicted true positive instances as those having prediction boxes with an intersection over union (IoU) value of 0.7 or greater when compared to the corresponding ground truth boxes. During the evaluation process, we exclude the boxes with scores that fall below 0.1. It is essential to note

TABLE III: The performances of different 3D object detection algorithms in the urban scenario under repetitive and non-repetitive LiDAR scanning patterns.

		Pillar-based	Voxel-based	Transformer-based	
		Pillarnet	SECOND	CT3D	PDV
Non-repetitive	Car	78.47	78.82	87.33	85.94
	Cyclist	73.02	73.03	81.36	79.17
	Pedestrian	41.05	42.98	56.76	52.48
Repetitive	Car	77.97	77.90	86.62	85.26
	Cyclist	74.63	72.85	80.84	78.68
	Pedestrian	42.95	41.42	55.80	52.14
Delta $AP\|_{R_{40}}$	Car	**0.50**	**0.92**	**0.71**	**0.68**
	Cyclist	**-1.61**	**0.18**	**0.52**	**0.49**
	Pedestrian	**-1.9**	**1.56**	**0.96**	**0.34**

that the 3D object detection algorithms detect only a subset of the vehicles captured by the LiDAR.

The average precision (AP) is defined as:

$$AP = \frac{1}{40} \sum_{r \in R} \frac{TP}{TP + FP} \tag{1}$$

where we use the "$AP|_{R_{40}}$" to calculate the "AP." The "R" represents a recall set containing 40 sequential recall points, and the "FP" represents the number of false positive estimated objects, mainly vehicles in this section.

Figure 5 illustrates the performance of five 3D object detection algorithms in highway scenarios using both repetitive and non-repetitive LiDAR point cloud data. With the exception of point-based algorithms, the remaining algorithms exhibit similar performance on both types of LiDAR point cloud data. Due to the significantly lower absolute accuracy of point-based algorithms, they are excluded from subsequent discussions. Therefore, it can be concluded that the algorithm performance is not sensitive to the LiDAR scanning pattern as long as it meets a certain level of accuracy. Additionally, based on the results, the accuracy of different algorithm types can be categorized into three levels, with transformer-based methods demonstrating the highest accuracy.

2) Urban Scenario: In the urban scenario, we need to focus on three categories: vehicles, cyclists, and pedestrians. During our experiment, we divided the entire dataset into 5202 training frames and 2596 testing frames. The remaining 202 frames were excluded from the algorithm testing stage because they did not contain any objects within the specified range. In the urban scenario, due to the demand for accuracy, we provided the detection results for four 3D object detection models, using AP as the evaluation metric. Similar to the highway scenario, we considered predicted true positive samples as those prediction boxes with an IoU value of 0.7 or higher with the ground truth boxes, excluding boxes with scores below 0.1 during evaluation.

Table III presents the performance of four 3D object detection algorithms on both repetitive and non-repetitive LiDAR point cloud data in urban scenarios. Detection is conducted for three categories: vehicles, cyclists, and pedestrians. Similar to the highway scenario, various 3D object detection algorithms showcase comparable performance on both types of LiDAR scanning patterns, with accuracy differences of nearly less than one point. Consequently, we can draw the following conclusions:

1) The scanning pattern of LiDAR does not influence the performance of 3D object detection algorithms. These models can be trained consistently across various categories, producing similar results regardless of the LiDAR scanning pattern.
2) Transformer-based methods indeed exhibit the highest performance in the 3D object detection task, while voxel and pillar-based methods demonstrate satisfactory accuracy. In contrast, point-based methods exhibit the lowest accuracy.

TABLE IV: Domain gap of repetitive and non-repetitive LiDAR scanning patterns in the highway scenario.

	Point-based	Pillar-based	Voxel-based	Transformer-based	
	PointRCNN	Pillarnet	SECOND	CT3D	PDV
Repetitive	52.28	82.71	82.91	88.42	89.20
Non-repetitive	42.04	75.32	76.17	85.94	86.08
Delta $AP\|_{R_{40}}$	**10.24**	**7.39**	**6.74**	**2.48**	**3.12**

B. Domain Gap Between Different LiDAR Scanning Patterns

Since the current mainstream datasets are collected from repetitive LiDAR, there is a lack of diverse non-repetitive data resources to train models, which may lead to some safety issues in autonomous driving. To solve this problem, due to the consistency of the point cloud structure, one possible solution is to pre-train models using the rich data from repetitive LiDAR, and then use the pre-trained model for training and inference on non-repetitive data. To assess the feasibility of this approach, we tested the migration ability of different algorithms between different LiDAR scanning patterns and derived the domain gap resulting from different scanning patterns. It is important to note that our datasets for different LiDARs were collected under the same conditions and scenarios. Therefore, the domain differences we observed were solely due to the effects of different scanning patterns of LiDAR. During our experiments, we trained different models on the repetitive point cloud data training set and then tested them on both the repetitive and non-repetitive test sets. This helped us to determine the difference in performance of the same model on two different test sets. We used this accuracy degradation to represent the effect of different scanning patterns on the domain differences and the different migration abilities of various 3D object detection algorithms.

1) Highway Scenario: Table IV demonstrates the migration ability of different algorithms on the vehicle category in the highway scenario, using the AP difference as an evaluation metric. The various types of 3D object detection algorithms do show a certain degree of accuracy degradation with an average value of 6 points. This reflects the presence of domain differences between the point clouds collected by

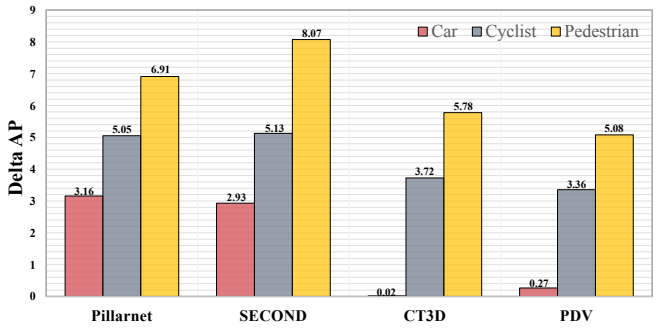

Fig. 6: Domain gap of repetitive and non-repetitive LiDAR scanning patterns in the urban scenario.

different LiDAR scanning patterns. Further analysis shows that the point-based algorithm exhibits the largest accuracy degradation, and the transformer-based method displays the smallest accuracy degradation.

2) Urban Scenario: In the urban scenario, we investigate the accuracy degradation of the three categories of vehicles, cyclists, and pedestrians. Figure 6 shows the migration ability of different algorithms on the three categories, as well as the corresponding domain differences of the three categories. The results indicate that the pedestrian category exhibits the largest domain gap, while the vehicle category exhibits the smallest domain gap. Regarding the different algorithm categories, the pillar-based and voxel-based methods show significant accuracy degradation in each category. Conversely, the transformer-based method demonstrates minimal accuracy degradation overall and even achieves zero degradation in accuracy within the vehicle category. So we can draw the following conclusions:

1) Different scanning patterns do indeed result in a noticeable domain difference in the point clouds collected by LiDARs. Moreover, as the size of the object decreases, the domain gap tends to widen.
2) Transformer-based methods exhibit superior migration ability between repetitive and non-repetitive scanning patterns. This capability enables the domain adaptation from repetitive data to non-repetitive data.

VI. Conclusion and Future Works

In general, this paper investigates two scanning patterns of LiDAR: repetitive and non-repetitive, and their impact on LiDAR scanning abilities and the performance of 3D object detection algorithms, as well as the domain gap generated by different scanning patterns. Based on these two commonly used LiDAR scanning patterns in current production vehicles, we collected the "Repetitive-or-not" dataset under the same installation conditions and identical acquisition scenarios. Through the comprehensive analysis of the "Repetitive-or-not" dataset, we observed that non-repetitive LiDAR exhibits stronger scanning abilities, capturing more high-quality objects from the environment, especially smaller objects that are hard to capture. Moreover, the performance of 3D object detection algorithms is not significantly affected by different scanning patterns. Finally, through experiments, we conclude that there is a certain domain gap between point cloud data obtained from LiDARs with different scanning patterns, and different kinds of algorithms exhibit certain differences in migration abilities.

Based on the findings from the above research, we can draw the following conclusions:

1) Non-repetitive LiDAR holds great promise for the future. Given the near-identical performance of 3D object detection algorithms between repetitive and non-repetitive point clouds, utilizing non-repetitive data is indeed likely to result in the detection of more objects. This is because LiDARs employing this scanning pattern demonstrate an enhanced capability to capture high-quality objects in various scenarios. Moreover, non-repetitive LiDARs typically have a lower price than repetitive LiDARs, showcasing their practical cost-effectiveness in real-world scenarios.
2) Transformer-based methods indeed emerge as the top performers in 3D object detection tasks among all algorithm types. Furthermore, they exhibit the strongest migration abilities, enabling them to maximize the utilization of point cloud data collected by both repetitive and non-repetitive LiDARs.

It is important to note that the conclusions drawn from this experiment are based on the same configuration for both non-repetitive and repetitive LiDAR. However, as shown in Table I, the hardware specifications of repetitive LiDAR are better than those of non-repetitive LiDAR, and the number of points generated by repetitive LiDAR will be greater. In this research, we mainly aim to demonstrate the effects of two different scanning patterns, non-repetitive and repetitive, on the LiDAR scanning ability under the same conditions, as well as their respective advantages and disadvantages. In subsequent research, we remain committed to exploring the impact of time deskewing of 3D scans on the two scanning patterns. Additionally, we continue to introduce various scanning tasks in more challenging conditions to further explore the scanning potential of non-repetitive LiDAR. In the future, with the advancement of LiDAR production technology, we believe that non-repetitive, as a promising scanning pattern, will be put into more practical applications.

References

[1] R. Roriz, J. Cabral, and T. Gomes, "Automotive lidar technology: A survey," *IEEE Transactions on Intelligent Transportation Systems*, vol. 23, no. 7, pp. 6282–6297, 2022.
[2] A. Geiger, P. Lenz, C. Stiller, and R. Urtasun, "Vision meets robotics: The kitti dataset," *International Journal of Robotics Research (IJRR)*, 2013.
[3] H. Caesar, V. Bankiti, A. H. Lang, S. Vora, V. E. Liong, Q. Xu, A. Krishnan, Y. Pan, G. Baldan, and O. Beijbom, "nuScenes: A multimodal dataset for autonomous driving," in *Proceedings of the IEEE/CVF Conference on Computer Vision and Pattern Recognition (CVPR)*, 2020, pp. 11 621–11 631.
[4] P. Sun, H. Kretzschmar, X. Dotiwalla, A. Chouard, V. Patnaik, P. Tsui, J. Guo, Y. Zhou, Y. Chai, B. Caine *et al.*, "Scalability in perception for autonomous driving: Waymo open dataset," in *Proceedings of the IEEE/CVF Conference on Computer Vision and Pattern Recognition (CVPR)*, 2020, pp. 2446–2454.

[5] A. Dosovitskiy, G. Ros, F. Codevilla, A. Lopez, and V. Koltun, "Carla: An open urban driving simulator," in *Conference on Robot Learning*. PMLR, 2017, pp. 1–16.

[6] Y. Zhou and O. Tuzel, "Voxelnet: End-to-end learning for point cloud based 3D object detection," in *Proceedings of the IEEE/CVF Conference on Computer Vision and Pattern Recognition (CVPR)*, 2018, pp. 4490–4499.

[7] Y. Yan, Y. Mao, and B. Li, "Second: Sparsely embedded convolutional detection," *Sensors*, vol. 18, no. 10, p. 3337, 2018.

[8] A. H. Lang, S. Vora, H. Caesar, L. Zhou, J. Yang, and O. Beijbom, "Pointpillars: Fast encoders for object detection from point clouds," in *Proceedings of the IEEE/CVF Conference on Computer Vision and Pattern Recognition (CVPR)*, 2019, pp. 12 697–12 705.

[9] G. Shi, R. Li, and C. Ma, "Pillarnet: Real-time and high-performance pillar-based 3d object detection," in *Proceedings of the European Conference on Computer Vision (ECCV)*, 2022, pp. 35–52.

[10] S. Shi, X. Wang, and H. Li, "Pointrcnn: 3d object proposal generation and detection from point cloud," in *Proceedings of the IEEE/CVF Conference on Computer Vision and Pattern Recognition (CVPR)*, 2019, pp. 770–779.

[11] T. Yin, X. Zhou, and P. Krahenbuhl, "Center-based 3D object detection and tracking," in *Proceedings of the IEEE/CVF Conference on Computer Vision and Pattern Recognition (CVPR)*, 2021, pp. 11 784–11 793.

[12] H. Sheng, S. Cai, Y. Liu, B. Deng, J. Huang, X.-S. Hua, and M.-J. Zhao, "Improving 3d object detection with channel-wise transformer," in *Proceedings of the IEEE/CVF International Conference on Computer Vision (ICCV)*, 2021, pp. 2743–2752.

[13] C. R. Qi, O. Litany, K. He, and L. J. Guibas, "Deep hough voting for 3d object detection in point clouds," in *Proceedings of the IEEE/CVF International Conference on Computer Vision (ICCV)*, 2019, pp. 9277–9286.

[14] I. Misra, R. Girdhar, and A. Joulin, "An end-to-end transformer model for 3d object detection," in *Proceedings of the IEEE/CVF International Conference on Computer Vision (ICCV)*, 2021, pp. 2906–2917.

[15] C. R. Qi, X. Chen, O. Litany, and L. J. Guibas, "Imvotenet: Boosting 3d object detection in point clouds with image votes," in *Proceedings of the IEEE/CVF Conference on Computer Vision and Pattern Recognition (CVPR)*, 2020, pp. 4404–4413.

[16] Y. Zheng, Y. Duan, J. Lu, J. Zhou, and Q. Tian, "HyperDet3D: Learning a Scene-conditioned 3D Object Detector," in *Proceedings of the IEEE/CVF Conference on Computer Vision and Pattern Recognition (CVPR)*, 2022, pp. 5585–5594.

[17] J. Deng, S. Shi, P. Li, W. Zhou, Y. Zhang, and H. Li, "Voxel r-cnn: Towards high performance voxel-based 3D object detection," in *Proceedings of the AAAI Conference on Artificial Intelligence (AAAI)*, vol. 35, no. 2, 2021, pp. 1201–1209.

[18] H. Kuang, B. Wang, J. An, M. Zhang, and Z. Zhang, "Voxel-FPN: Multi-scale voxel feature aggregation for 3D object detection from LiDAR point clouds," *Sensors*, vol. 20, no. 3, p. 704, 2020.

[19] S. Shi, C. Guo, L. Jiang, Z. Wang, J. Shi, X. Wang, and H. Li, "Pv-rcnn: Point-voxel feature set abstraction for 3d object detection," in *Proceedings of the IEEE/CVF Conference on Computer Vision and Pattern Recognition (CVPR)*, 2020, pp. 10 529–10 538.

[20] S. Shi, L. Jiang, J. Deng, Z. Wang, C. Guo, J. Shi, X. Wang, and H. Li, "PV-RCNN++: Point-voxel feature set abstraction with local vector representation for 3D object detection," *International Journal of Computer Vision*, vol. 131, no. 2, pp. 531–551, 2023.

[21] W. Yan, Y. Qian, C. Wang, and M. Yang, "Threshold-adaptive unsupervised focal loss for domain adaptation of semantic segmentation," *IEEE Transactions on Intelligent Transportation Systems*, vol. 24, no. 1, pp. 752–763, 2023.

[22] G. Zamanakos, L. Tsochatzidis, A. Amanatiadis, and I. Pratikakis, "A comprehensive survey of LiDAR-based 3D object detection methods with deep learning for autonomous driving," *Computers & Graphics*, vol. 99, pp. 153–181, 2021.

[23] C. R. Qi, H. Su, K. Mo, and L. J. Guibas, "Pointnet: Deep learning on point sets for 3d classification and segmentation," in *Proceedings of the IEEE Conference on Computer Vision and Pattern Recognition (CVPR)*, 2017, pp. 652–660.

[24] D. Lu, Q. Xie, M. Wei, L. Xu, and J. Li, "Transformers in 3D point clouds: A survey," *arXiv preprint arXiv:2205.07417*, 2022.

[25] A. Geiger, P. Lenz, C. Stiller, and R. Urtasun, "Vision meets robotics: The kitti dataset," *The International Journal of Robotics Research*, vol. 32, no. 11, pp. 1231–1237, 2013.

[26] J. Mao, M. Niu, C. Jiang, H. Liang, J. Chen, X. Liang, Y. Li, C. Ye, W. Zhang, Z. Li *et al.*, "One million scenes for autonomous driving: Once dataset," *arXiv preprint arXiv:2106.11037*, 2021.

[27] A. Patil, S. Malla, H. Gang, and Y.-T. Chen, "The h3d dataset for full-surround 3d multi-object detection and tracking in crowded urban scenes," in *Proceedings of the IEEE International Conference on Robotics and Automation (ICRA)*, 2019, pp. 9552–9557.

[28] M.-F. Chang, J. Lambert, P. Sangkloy, J. Singh, S. Bak, A. Hartnett, D. Wang, P. Carr, S. Lucey, D. Ramanan *et al.*, "Argoverse: 3d tracking and forecasting with rich maps," in *Proceedings of the IEEE/CVF Conference on Computer Vision and Pattern Recognition (CVPR)*, 2019, pp. 8748–8757.

[29] I. Kim, R. J. Martins, J. Jang, T. Badloe, S. Khadir, H.-Y. Jung, H. Kim, J. Kim, P. Genevet, and J. Rho, "Nanophotonics for light detection and ranging technology," *Nature Nanotechnology*, vol. 16, no. 5, pp. 508–524, 2021.

[30] J. Lemmetti, N. Sorri, I. Kallioniemi, P. Melanen, and P. Uusimaa, "Long-range all-solid-state flash LiDAR sensor for autonomous driving," in *Proceedings of High-Power Diode Laser Technology*, vol. 11668. SPIE, 2021, pp. 99–105.

[31] C. V. Poulton, M. J. Byrd, P. Russo, E. Timurdogan, M. Khandaker, D. Vermeulen, and M. R. Watts, "Long-range lidar and free-space data communication with high-performance optical phased arrays," *IEEE Journal of Selected Topics in Quantum Electronics*, vol. 25, no. 5, pp. 1–8, 2019.

[32] D. Wang, S. Strassle, A. Stainsby, Y. Bai, S. Koppal, and H. Xie, "A compact 3d lidar based on an electrothermal two-axis mems scanner for small uav," in *Laser Radar Technology and Applications XXIII*, vol. 10636. SPIE, 2018, pp. 93–99.

[33] T. Raj, F. Hanim Hashim, A. Baseri Huddin, M. F. Ibrahim, and A. Hussain, "A survey on lidar scanning mechanisms," *Electronics*, vol. 9, no. 5, p. 741, 2020.

[34] J. Sun, E. Timurdogan, A. Yaacobi, E. S. Hosseini, and M. R. Watts, "Large-scale nanophotonic phased array," *Nature*, vol. 493, no. 7431, pp. 195–199, 2013.

[35] N. Koenig and A. Howard, "Design and use paradigms for gazebo, an open-source multi-robot simulator," in *2004 IEEE/RSJ international conference on intelligent robots and systems (IROS)(IEEE Cat. No. 04CH37566)*, vol. 3. Ieee, 2004, pp. 2149–2154.

[36] J. S. Hu, T. Kuai, and S. L. Waslander, "Point density-aware voxels for lidar 3d object detection," in *Proceedings of the IEEE/CVF Conference on Computer Vision and Pattern Recognition (CVPR)*, 2022, pp. 8469–8478.